Original Article

Inhalation lung injury induced by smoke bombs in children: CT manifestations, dynamic evolution features and quantitative analysis

Yaqiong Ma[1#], Shikui Zhang[2#], Lianping Zhao[1], Xing Zhou[1], Zeqing Mao[1], Huaxin Xu[1], Xiaorui Ru[1], Gang Huang[1]

[1]Department of Radiology, [2]Department of Emergency, Gansu Provincial Hospital, Lanzhou 713000, China

Contributions: (I) Conception and design: G Huang; (II) Administrative support: G Huang, Y Ma; (III) Provision of study materials or patients: Y Ma, S Zhang; (IV) Collection and assembly of data: Y Ma, S Zhang, H Xu; (V) Data analysis and interpretation: All authors; (VI) Manuscript writing: All authors; (VII) Final approval of manuscript: All authors.

[#]These authors contributed equally to this work.

Correspondence to: Professor Gang Huang. Department of Radiology, Gansu Provincial Hospital, Donggang Road No. 204, Cheng-Guan District, Lanzhou 730030, China. Email: keen0999@163.com.

Background: This retrospective study aimed to investigate the computed tomography (CT) manifestations, short-term dynamic evolution features and quantitative lung CT analysis of inhalation lung injury induced by smoke bomb flare.

Methods: Eleven pediatric patients (aged 11 to 13) who inhaled the smoke of smoke bombs underwent several low-dose chest CT scans. The image characteristics and their dynamic changes were observed and quantitative CT values were analyzed. The quantitative CT indicators included lung injury CT score (LICTS), lung fibrosis CT score (LFCTS), mean lung density (MLD), normally aerated volume ratio (NAVR) and reductively aerated volume ratio (RAVR). Box-plot was used to analyze the dynamic changes of each indicator and Spearman statistical method was used to analyze the correlation between any two indicators.

Results: (I) In most cases, there were multiple consolidation and massive ground-glass opacities (GGOs) in the two lungs, which aggravated in the early stage and then gradually dissoluted in the later stage. LICTS was positively correlated with MLD (r=0.811, P=0.000), while it was negatively correlated with NAVR (r=–0.712, P=0.000). There existed interstitial fibrosis in the later stage, and LFCTS was positively correlated with RAVR (r=0.382, P=0.028). (II) In one case, the patterns were like layered cake, i.e., consolidation with air bronchus signs in the accumulation area, GGOs in the aforementioned area and normal lung in the top area. The patterns aggravated in the early stage and quickly dissolved in the later stage, and only a few residual fibrotic lesions existed on the final scan. (III) For severe cases, pneumomediastinum and subcutaneous emphysema aggravated in the early stage and then gradually dissolved in the later stage.

Conclusions: The chest CT manifestations of inhalation lung injury induced by smoke bombs are predominantly GGOs and consolidation. They aggravate in the early stage and gradual dissolute in the later stage. CT quantitative values can contribute to evaluating the extent of this disease, and NAVR and RAVR can be used to assess pulmonary function.

Keywords: Computed tomography (CT); inhalation lung injury; dynamic evolution; quantitative analysis; smoke bombs; children

Submitted Jun 08, 2018. Accepted for publication Sep 10, 2018.
doi: 10.21037/jtd.2018.09.84
View this article at: http://dx.doi.org/10.21037/jtd.2018.09.84

Introduction

Smoke bombs are often used in military/fire drills, firefighter training, and on the battlefield as obscurants. Smoke bombs can release a mixed chemical smoke containing zinc chloride, zinc oxide, hexachloroethane and other chemical ingredients after flaring. Smoke inhaling can cause airway and lung injury. Pathological changes of this inhalation lung injury include edema of interstitial and alveolar, an increase of fibroblasts as well as an increase of collagen in the interstitium and alveolus in the early phase, and pulmonary fibrosis in the later phase (1,2). A number of studies have already focused on clinical, radiographic, and pulmonary function of smoke inhalation (3-7). Some studies showed that the chest radiograph is an insensitive indicator of inhalation of airway and parenchymal lung injury (8,9). Therefore, computed tomography (CT) was used by radiologists to diagnose the inhalation lung injury. Compared with the chest radiograph, CT is more reliable for the detection of pulmonary abnormalities at an early stage, as also for the demonstration of pulmonary complications during the follow-up (10). There was a study to evaluate the efficacy of CT scan in assessing the severity of inhalation lung injury with sheep, and the conclusion was that CT scan was potentially useful in gauging the severity of inhalation injury non-invasively (11). In recent years, quantitative CT has been used in the evaluation of lung fibrosis (12-15). Therefore, the authors would like to study whether CT quantitative analysis can be used to further evaluate the severity and longitudinal changes of inhalation lung injury.

A rare opportunity was obtained to study the CT findings of smoke inhalation lung injury in children in the tragic accident of Tianshui Yifu Primary School in Gansu province, which practiced the fire drill on September 18, 2015. Most children developed vomiting, chest distress, shortness of breath, dyspnea, asphyxia, coma, hemoptysis, hemafecia and other symptoms. Through observing and studying the clinical manifestations, laboratory test results, chest CT manifestations and short-term prognosis of these 11 pediatric patients, it was found that the main abnormalities were demonstrated on chest CT. At the same time, CT quantitative analysis was employed to get more diagnostic information, especially to evaluate interstitial fibrosis in the later stage. The findings might help in treating smoke bomb poisoning, improving prognosis, and especially benefiting children in a war area and soldiers in a war or in military drills.

Methods

This retrospective study aimed to investigate the CT manifestations, short-term dynamic evolution features and quantitative lung CT analysis of inhalation lung injury induced by smoke bomb flare. CT scores were evaluated by two radiologists. Lung volume was obtained by CT post-processing station. In this study, combining these two methods to assess the extent of main abnormalities during the course of inhalation lung injury could help make the results more objective. In addition, lung volume indicators were also used to evaluate the pulmonary function of this disease.

Patients

All patients injured in this accident were healthy primary school pupils. The 11 pediatric patients treated in Gansu Provincial Hospital were transferred from the local hospital in Tianshui city after receiving treatment for 3 days. Among these 11 patients, there were seven males and four females. Two patients were 11 years old; seven patients were 12 years old, and two patients were 13 years old. The condition of the 11 patients improved, and they were discharged after receiving treatment for 24–50 days in Gansu Provincial Hospital.

Because delayed-onset noncardiogenic pulmonary edema may develop 12 to 72 hours later, longer observation period has been recommended for people with significant exposure to low solubility agents (16-18), and the sensitivity of CT in finding the abnormalities of inhalation lung injury is higher than that of the chest radiograph (10). Therefore, to observe the changes of this disease, the patients underwent several low-dose CT scans. This decision came from multi-disciplinary team (MDT) at that time. The examination and treatment complied with our local ethical guidelines approved by the Institutional Ethics Review Board of Gansu Provincial Hospital (approval number 2015-071).

CT images acquisition and interpretation

A GE VCT scanner (General Electric Medical Systems, USA) was used to scan all the patients. Scans were obtained at full inspiration from the apex to the lung base with the patients in the supine position. The following parameters were adopted: tube voltage 100 kV, tube current 150–250 mA (automatic), scanning range 25–30 cm, slice thickness 5 mm, and with 0.6 mm thin-section reconstructions

Table 1 The values of each indicator in five CT scans (mean ± SD)

Indicator	1 (Sep 22nd)	2 (Sep 24th)	3 (Oct 1st)	4 (Oct 8th)	5 (Oct 15th)
LICTS	20.11±1.51	20.45±1.81	14.55±5.37	7.00±2.32	1.09±1.04
LFCTS	–	–	2.45±1.21	9.64±2.84	6.82±2.23
MLD	−640.91±40.27	−640.19±68.15	−693.45±73.40	−720.20±35.91	−771.64±30.00
NAVR (%)	10.42±8.56	9.47±11.17	22.57±20.81	21.13±14.23	42.10±13.83
RAVR (%)	28.90±6.27	29.30±10.56	29.05±9.10	38.44±8.26	30.78±8.58

LICTS, lung injury CT score; LFCTS, lung fibrosis CT score; MLD, mean lung density; NAVR, normally aerated volume ratio; RAVR, reductively aerated volume ratio; CT, computed tomography.

using a standard algorithm, dose length product 105.58± 20.32 mGy-cm, and effective dose 1.79±0.35 mSv [k value referred to the quality criteria for CT developed by the Commission of the European Communities (19), k_{thorax} =0.017 mSv/(mGy.cm). The scans were viewed with a window level of −700 Hounsfield units (HU) and width of 1,200–1,500 HU. The predominant patterns of the early stage on CT scan were categorized as ground-glass opacities (GGOs), consolidation, reticular pattern, and mixed pattern (combination of consolidation, GGOs, and reticular opacities). Then, it was noted that the predominant pattern of later stage on CT scan included reticular pattern, septal thickening, intralobular lines, parenchymal bands and irregular lines superimposed on GGOs.

CT scores

Thin-section CT images were evaluated for the presence, distribution, and extent to get lung injury CT score (LICTS) and lung fibrosis CT score (LFCTS). The predominant patterns of LICTS: (I) GGOs; (II) consolidation; (III) mixed pattern (GGOs/consolidation, and reticular pattern). The predominant patterns of LFCTS: (I) reticular pattern; (II) septal lines; (III) parenchymal bands; (IV) mixed pattern (reticular pattern/septal lines/parenchymal bands, and subpleural ground glass opacity/ irregular linear opacities). Each lung was divided into three zones: upper (above the carina), middle (below carina up to the inferior pulmonary vein) and lower (below the inferior pulmonary vein). Each zone was evaluated for percentage of lung involvement based on the following band scores: (I) 0 score: normal; (II) 1 score: involvement of less than 25% of the images; (III) 2 score: 25% to 50%; (IV) 3 score: 50% to 75%; (4) 4 score: more than 75%. Summation of scores from all six lung zones provided the overall CT score (maximal CT score =24) that the above scoring method is based on and modified the protocol from the following study (20,21). Two experienced radiologists (G Huang, X Zhou), both of whom had more than 10 years of experience in thoracic radiology, reviewed the thin-section CT images and reached a conclusion in consensus.

Measurement of lung volume

The integrated lung quantification software of AW 4.4 workstation was used to measure the lung volume to evaluate the pulmonary function. The pulmonary parenchyma was divided into four regions based on the ranges of Hounsfield unit (HU) reported by Gattinoni *et al.* (22,23): hyperinflated areas (−1,024 to −901 HU), normally aerated areas (−900 to −801 HU), reductively aerated areas (−800 to −701 HU), and restricted ventilation areas (<−700 HU) were defined by the software for each of the lungs. The software also generated the total lung volume and mean lung density (MLD). In order to decrease the individual bias, normally aerated volume ratio (NVAR) and reductively aerated volume ratio (RAVR) were used, which means normally aerated volume and reductively aerated volume was divided by total lung volume respectively.

Statistical analysis

Box-plot and Spearman statistical methods were used with SPSS 17.0 (SPSS, IL, USA). The detailed values and dynamic changes were presented in *Table 1* and *Figure 1A,B,C,D,E.*

Results

Clinical parameters

The pediatric patients sent to Gansu Provincial Hospital

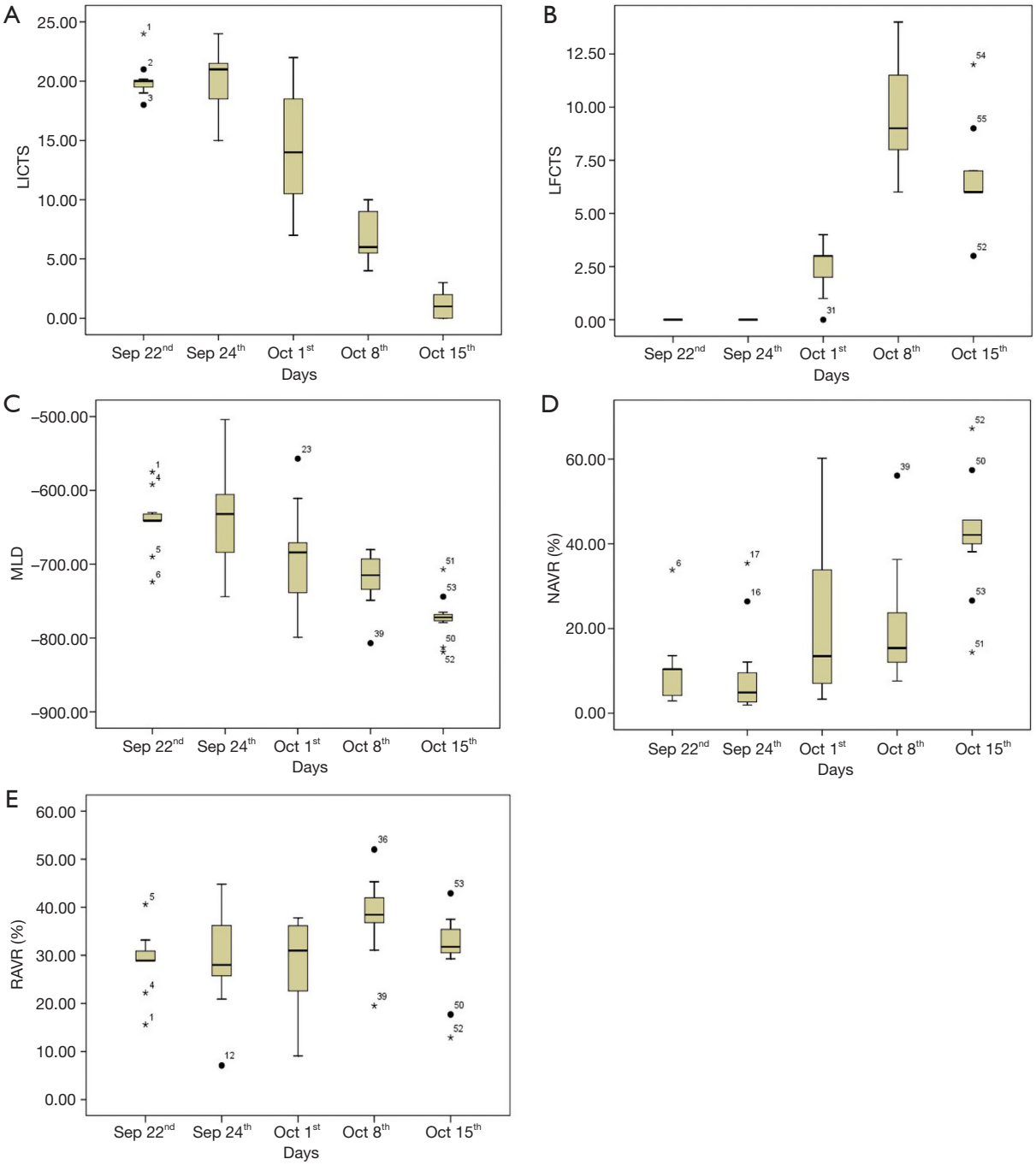

Figure 1 Changes in LICTS (A), LFCTS (B), MLD (C), NAVR (D) and RAVR (E) from the time of the initial scan to the follow-up. LICTS, lung injury CT score; LFCTS, lung fibrosis CT score; MLD, mean lung density; NAVR, normally aerated volume ratio; RAVR, reductively aerated volume ratio; CT, computed tomography.

were all classified as "severe" in the local hospital. Most of them had vomiting (n=11), chest distress (n=11), shortness of breath (n=11), dyspnea (n=11), asphyxia (n=3), coma (n=2), hemoptysis (n=4) and hemafecia (n=4). All the patients were given timely oxygen therapy, anti-inflammatory, and other treatments in the local hospital after the accident. Only one patient with the worst condition had increased white blood cells [12.745×10^9/L (normal range, 4×10^9–10×10^9/L)]. Three patients had increased neutrophils [78%, 85%, 97% (normal range, 50–70%)]. Other blood test indicators were within normal range. Since all the children were admitted to the intensive care unit, no pulmonary function test was conducted, as it is not advisable to conduct such tests during the acute phase. Serial CT scans were obtained at the time of hospitalization in Gansu Provincial Hospital. The indications for serial scans included clinical deterioration (n=11) and necessity of a change in treatment, whether it involved increased dosage of antibiotics (n=9) or anti-fibrotic therapy (n=11). In some patients, the first CT scans were also obtained to confirm the injury when radiographs obtained at presentation was normal or slightly abnormal (n=2). The condition in all patients deteriorated within 3 days after the first CT scans were obtained, and the second CT scans were thus obtained. From the second to the fifth scan, each scan was conducted with a seven-day interval so as to keep track of the progress of the patients' conditions. Five patients developed pneumomediastinum, with three of them also developing pneumothorax, two of them also developing subcutaneous pneumatosis during the 1st and 2nd week of evaluation. Over the course of treatment in these pediatric patients, all patients experienced aggravated dyspnea during the 1st week after the accident, which then gradually eased in the second week. However, shortness of breath again appeared in the patients in the 3rd week, and then the symptom gradually alleviated after anti-fibrotic therapies. In addition, the patient with the most severe condition was treated with endotracheal intubation and pneumothorax drain.

CT manifestations and the dynamic evolution features

Table 1 shows the values of each indicator in five CT scans (mean ± SD). There was a significant aggravation in the extent of this injury from the 4th day to the 7th day after the accident, and the median of LICTS of these two CT scans (22nd and 24th, Sep) were 20 (range, 18–24) and 21 (range, 18–24) respectively. After that, the extent decreased slowly to a median of LICTS of 14 (range, 7–22) from the 3rd CT images (1st, Oct) and 6 (range, 4–10) from the 4th CT images (8th, Oct), and 1 (range, 0–3) from the last CT images (15th, Oct), and this decrease reflected the effectiveness of anti-inflammatory therapy. The predominant patterns of abnormality changed over time. According to the 1st CT images, the main abnormalities included GGOs (10 out of 11 pediatric patients) and consolidation (8 out of 11 pediatric patients) (*Figure 2A*), then the scope of the abnormality expanded (*Figure 2B*). GGOs with consolidation were most commonly found from the 2nd CT images. According to the 3rd CT images, a combination of reticular pattern and parenchymal bands was noted in association with GGOs (*Figure 2C*). According to the 4th CT images, irregular linear opacities and/or interlobular septal thickening were noted in association with subpleural GGOs (10 out of 11 pediatric patients) (*Figure 2D*). Lung interstitial changes were found in these pediatric patients with the aid of the CT images on the 14th day (1st, Oct) after the accident and subsequently developed interstitial fibrosis and reached the highest proportions on the 21st day (8th, Oct), and these lesions were mostly distributed under the dorsal pleura (*Figure 2E,F,G*). The final CT scan was obtained on the 28th day (15th, Oct). It was noted that lung fibrosis significantly improved (*Figure 2H*). The median of LFCTS of these three CT scans (1st, 8th and 15th, Oct) were 3 (range, 0–4), 9 (range, 6–14) and 6 (range, 3–12) respectively. In one patient, the initial scan showed patterns like layered cake, consolidation with air bronchus signs in the accumulation area, GGOs in the aforementioned area, and normal lung in the top area. Conditions aggravated in the early stage, and there was quick dissolution in the later stage. Consolidation and GGOs resolved completely, and only a few residual fibrotic lesions were noted on the final scan (*Figure 3A,B*). Pneumomediastinum, subcutaneous emphysema, or pneumothorax were found in five patients on the 4th day after the accident (*Figure 4A,B*), which aggravated in the early stage and disappeared in the later stage.

Correlation analysis between lung volume and CT scores

Figure 1 shows the five quantitative indicators of five CT scans. From *Figure 1A*, the statistical value of the LICTS of each scan and the changes of the LICTS among the five scans can be seen. Similarly, *Figure 1B,C,D,E* show the statistical values of LFCTS, MLD, NVAR and RAVR respectively.

The correlations between MLD, NAVR or RAVR and

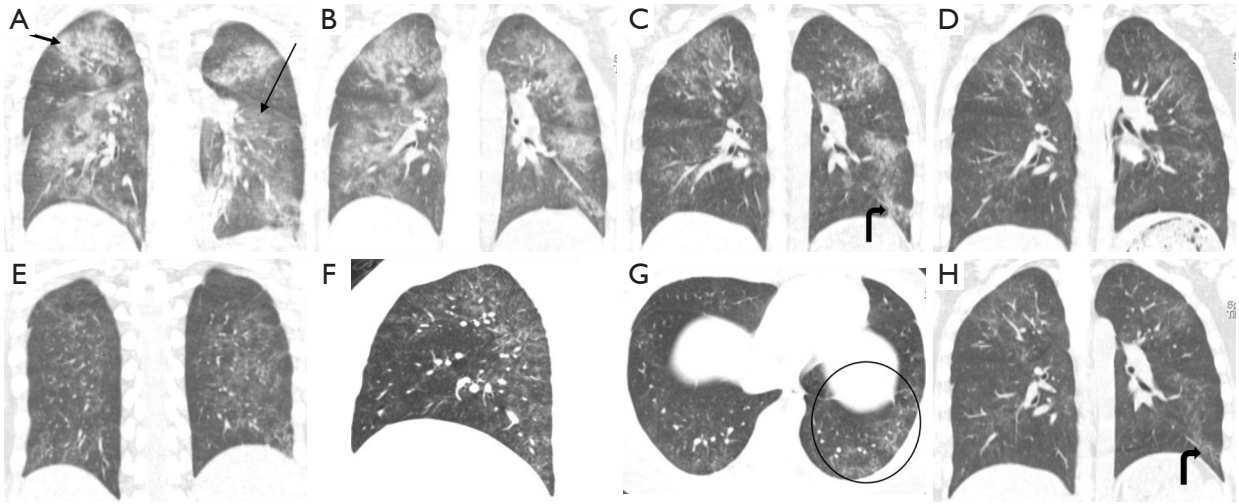

Figure 2 Five CT scans were obtained 4 days (A), 7 days (B), 14 days (C), 21 days (D,E,F,G) and 28 days (H) after smoke inhalation in a patient (female, 12 years old) showing GGOs (black long arrowhead) and consolidation (black short arrowhead) aggravated in the early stage and resolved in the later stage from the same coronal level (A-D,H), and then some parenchymal bands (curved arrowhead), irregular linear opacities and interlobular septal thickening with subpleural ground-glass opacities (circle) were left behind under the dorsal pleura. CT, computed tomography.

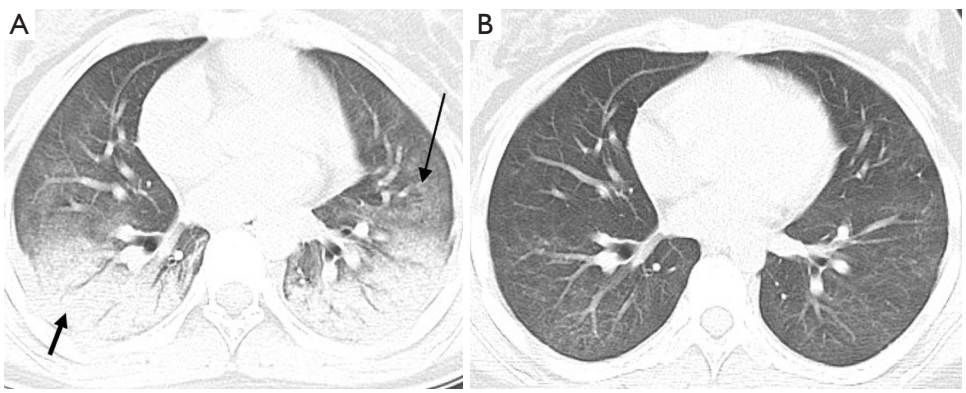

Figure 3 The 2nd CT scan (A) in a patient (female, 12 years old) shows the patterns are like layered cake, and the last CT scan (B) shows consolidation and GGOs resolved completely and there are only a few residual fibrotic lesions. CT, computed tomography; GGO, ground-glass opacity.

LICTS or LFCTS were analyzed by Spearman statistical method. The results of statistical differences are as follows: LICTS positively correlates with MLD (r=0.811, P=0.000), but negatively correlates with NVAR (r=–0.712, P=0.000); LFCTS positively correlates with RAVR (r=0.382, P=0.028) in the latter three CT scans.

Discussion

The serial scans obtained in Gansu Provincial Hospital provided an opportunity to study the longitudinal changes in inhalation lung injury induced by smoke bombs in the acute and convalescent periods. These children with the similar age inhaled the smoke at the same time and suffered nearly the same duration of exposure. Moreover, they were all classified as "severe" in the local hospital. Therefore, their conditions were basically similar when they were admitted to Gansu Provincial hospital. Several scans were made to help with treatment, which were the same in timing and interval of follow-up. The scans depicted the

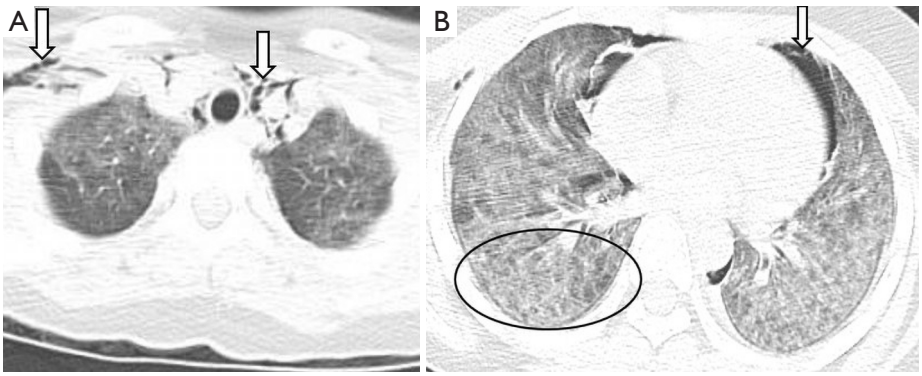

Figure 4 The 2nd CT scan in a patient (male, 13 years old) shows pneumomediastinum, subcutaneous emphysema, pneumothorax (white arrowhead) (A,B), and reticular patterns (oval) with excessive GGOs (B). CT, computed tomography; GGO, ground-glass opacity.

lung abnormalities at specific time points after the accident. To our knowledge, clinical, radiographic, and pathological findings, as well as treatment in patients who were exposed to smoke bombs, had been studied previously (1,2,24-27). However, to date, this is the first report of a longitudinal CT series in a relatively large group of pediatric patients with inhalation lung injury induced by smoke bombs. Lung injury was found on thin-section CT scans on the first day of admission. The extent of these injuries in these pediatric patients aggravated severely during the 1st week after the accident, and it was followed by a slow decline during the 2nd week. Lung fibrosis could be detected in the subpleural in the 3rd week, then it became more diffused in the 4th week, and it gradually dissolved after treatment. However, there was residual fibrosis in the last CT images. Improvement of interstitial fibrosis and reduction of LFCTS were attributed to the timely anti-fibrosis treatment of methylprednisolone from MDT after MDT observed the interstitial changes from the third CT images. The predominant abnormalities of lung CT images and dynamic changes were in concordance with the former report about lung injury induced by smoke bombs (26), though the subjects of the report were young soldiers. In this study, these findings can be shown not only by the evaluation of lung injury and fibrosis CT scores, but also by the objective measurement of various lung volumes and MLD with CT post-processing software. Both methods combined to find the features and assess the extent of inhalation lung injury and subsequent fibrosis can be very helpful in the treatment and prognosis of this disease.

In this study, GGOs and consolidation were the predominant abnormalities of the lung inhalation injury induced by smoke bombs. Image findings were based on histological characteristics, which included pulmonary edema, alveolitis, interstitial fibrosis, intra-alveolar fibrosis and diffuse alveolar damage (1,28,29). The number of pediatric patients with GGOs was highest in the 1st week (10 out of 11 pediatric patients), which decreased in the following one week and had a moderate upsurge trend in the 3rd week. The upsurge trend was due to the appearance of subpleural ground glass opacity and irregular linear opacities. Another predominant pattern of consolidation was common in the 1st week (8 out of 11 pediatric patients), which decreased in the following two weeks and disappeared in the 4th week. The consolidation areas totally resolved or reduced to small areas of fine reticulation. The reticular pattern associated with subpleural parenchymal bands and septal lines was detected to increase progressively from the 3rd week. Apart from these findings, the final scans of all pediatric patients in the 4th week showed residual abnormalities, including reticular pattern or GGOs with a superimposed reticular pattern and septal lines. The image characteristics of the CT scans obtained from the 3rd to the 4th week were clarified as interstitial fibrosis. The parenchymal bands indicated subsegmental atelectasis, which would be reversed as a result of resolution of inflammation with re-expansion of alveoli. Similarly, the resolution of interstitial edema and cellular infiltration could also explain the resolution of subpleural irregular linear opacities and septal lines. In one patient, the initial scan showed patterns like layered cake, consolidation with air bronchus signs in the accumulation area, GGOs in the aforementioned area and normal lung in the top area. The final scan showed that consolidation and GGOs resolved completely, and that there were only a few residual fibrotic lesions. Therefore, it was speculated that large

and obvious consolidation accompanied with air bronchus signs was more easily resolved. The finding was similar to the CT images and prognosis of lobar pneumonia. Pneumomediastinum, subcutaneous emphysema or pneumothorax were found in five patients in the 4th day after the accident, which aggravated in the early stage and gradually resolved in the later stage. These findings were consistent with some former studies on adults (1,26,29,30). These conditions may be followed by severe cough caused by exposure to toxic materials such as chlorine (31) and nitrogen oxide (32). The mechanism of pneumothorax and pneumomediastinum may be the result of alveolar rupture caused by the direct injury of the alveoli (31).

Subsequently, CT scores were used to assess the extent of lung injury and fibrosis during the course of inhalation lung injury. Thus, the longitudinal changes of these two main abnormalities could be seen directly. Meanwhile, the integrated lung quantification software of AW 4.4 workstation was used to measure the lung volume to evaluate the lung function. It was found that LICTS positively correlated with MLD (r=0.811, P=0.000), while negatively correlated with NVAR (r=−0.712, P=0.000). Therefore, it was concluded that MLD can objectively measure the extent of lung injury, and which suggested that MLD combined with LICTS may be a reliable way to evaluate the severity of inhalation lung injury. With the increase of LICTS, NAVR decreased. Therefore, to some extent, NAVR could be used to predict the pulmonary function when pulmonary function tests were not done in the acute stage of inhalation lung injury. Meanwhile, a correlation was studied between LICTS and RAVR and a negative correlation was found (r=−0.445, P=0.001), but which was unexplainable from the perspective of modern medicine. So, why were there changes in RAVR, especially in the latter three CT scans? Because lung fibrosis was detected from the latter three CT scans, and it usually caused a restrictive ventilation disorder, it was thus hypothesized that there may be some relationship between RAVR and LFCTS, and just as expected, there was a positive correlation between RAVR and LFCTS (r=0.382, P=0.028) from the latter three CT scans. Therefore, it was speculated that RAVR can objectively detect the changes of pulmonary function resulting from lung fibrosis. It was believed that it would aid the adjustment of treatment timely because one important principle of lung fibrosis treatment was to give treatment when lung fibrosis was reversible so as to control the progress of the disease. When the authors referred to a study about HRCT scan findings and pulmonary function, it suggested that smoke bombs caused predominantly parenchymal damage of the lung and a restrictive type of functional impairment (26). The main manifestation of restrictive ventilation was the reduction in inhalation. Thus, it was concluded that increased RAVR as measured by the integrated lung quantification software was consistent with the restrictive type of functional impairment as evaluated by pulmonary function tests at the lung fibrosis stage of inhalation lung injury. PFTs were helpful for patients with inhalation lung injury, especially for follow-up surveys. In this study, NAVR and RAVR could also predict the changes in pulmonary function to certain extent for patients with inhalation lung injury without PFTs, especially for patients in acute phase and/or with low compliance (such as the pediatric patients). However, this deduction needs to be tested in a larger number of patients.

One year later, it was found that there were small calcification points scattered under the pleura in the child with the most severe conditions, and the rest of the children were with subtle fine lines under the lower lobe from the review images. Therefore, it was speculated that the lung fibrosis caused by inhalation lung injury was mostly reversible. However, because it was not a natural progression, it could not be excepted that lung fibrosis caused by inhalation lung injury was irreversible. Whether it was reversible or irreversible, this study showed that the earlier detection of lung fibrosis was and the earlier anti-fibrosis treatment was given, the better the prognosis would be.

These pediatric patients underwent five CT scans in a short period. Although they were taken according to the low-dose scan protocol, the effective radiation dose was still over the limit. It was necessary to observe the changes of the disease and adjust the treatment for the severe conditions of those patients at that time. The credibility of the government and the hospital was challenged and questioned due to the fire drill accident and the serial CT scans, but now that these things happened, the authors collected the related data to do a retrospective study to make more people get some lessons from this accident.

Conclusions

The CT scan features of inhalation lung injury induced by smoke bombs are predominantly GGOs and consolidation. Strong correlations are observed between LICTS and MLD or NAVR, and between LFCTS and RAVR in this study. These results suggest that inhaling the smoke from smoke bombs can cause parenchymal damage of the lung

in the early stage and lung fibrosis in the later stage, and that LICTS associated with MLD can be used to accurately evaluate the extent of lung injury. Meanwhile, NAVR can be used to assess the pulmonary function with lung injury, especially RAVR can be used to detect the changes of pulmonary function resulting from lung fibrosis so as to aid doctors to adjust treatment.

Acknowledgements

The authors thank Professor Lu Zhang of Xi'an International Studies University. The authors also thank Professor Xi-Ping Shen in Medical Statistics Department of Lanzhou University.
Funding: The study was supported by the scientific research fund of Gansu Provincial Hospital, the project number is 16GSSY1-7.

Footnote

Conflicts of Interest: The authors have no conflicts of interest to declare.

Ethical Statement: The study was approved by Institutional Ethics Review Board of Gansu Provincial Hospital (No. 2015-071).

References

1. Homma S, Jones R, Qvist J, et al. Pulmonary vascular lesions in the adult respiratory distress syndrome caused by inhalation of zinc chloride smoke: a morphometric study. Hum Pathol 1992;23:45-50.
2. Pettilä V, Takkunen O, Tukiainen P. Zinc chloride smoke inhalation: a rare cause of severe acute respiratory distress syndrome. Intensive Care Med 2000;26:215-7.
3. Fogarty PW, George PJ, Solomon M, et al. Long-term effects of smoke inhalation in survivors of the King's Cross underground station fire. Thorax 1991;46:914-8.
4. Large AA, Owens GR, Hoffman LA. The short-term effects of smoke exposure on the pulmonary function of firefighters. Chest 1990;97:806-9.
5. Liu D, Tager IB, Balmes JR, et al. The effect of smoke inhalation on lung function and airway responsiveness in wildland fire fighters. Am Rev Respir Dis 1992;146:1469-73.
6. Loke J, Farmer W, Matthay RA, et al. Acute and chronic effects of fire fighting on pulmonary function. Chest 1980;77:369-73.
7. Whitener DR, Whitener LM, Robertson KJ, et al. Pulmonary function measurements in patients with thermal injury and smoke inhalation. Am Rev Respir Dis 1980;122:731-9.
8. Putman CE, Loke J, Matthay RA, et al. Radiographic manifestations of acute smoke inhalation. AJR Am J Roentgenol 1977;129:865-70.
9. Wittram C, Kenny JB. The admission chest radiograph after acute inhalation injury and burns. Br J Radiol 1994;67:751-4.
10. Spyropoulou GA, Iconomou T, Tsagarakis M, et al. The value and prognostic role of the CT scan versus chest radiography in the follow-up of intubated burn patients with possible inhalation injury. Ann Burns Fire Disasters 2005;18:79-82.
11. Park MS, Cancio LC, Batchinsky AI, et al. Assessment of severity of ovine smoke inhalation injury by analysis of computed tomographic scans. J Trauma 2003;55:417-27.
12. Yabuuchi H, Matsuo Y, Tsukamoto H, et al. Evaluation of the extent of ground-glass opacity on high-resolution CT in patients with interstitial pneumonia associated with systemic sclerosis: comparison between quantitative and qualitative analysis. Clin Radiol 2014;69:758-64.
13. Kim HG, Tashkin DP, Clements PJ, et al. A computer-aided diagnosis system for quantitative scoring of extent of lung fibrosis in scleroderma patients. Clin Exp Rheumatol 2010;28:S26-35.
14. Kloth C, Maximilian Thaiss W, Preibsch H, et al. Quantitative chest CT analysis in patients with systemic sclerosis before and after autologous stem cell transplantation: comparison of results with those of pulmonary function tests and clinical tests. Rheumatology 2016;55:1763-70.
15. Salaffi F, Carotti M, Di Donato E, et al. Computer-Aided Tomographic Analysis of Interstitial Lung Disease (ILD) in Patients with Systemic Sclerosis (SSc). Correlation with Pulmonary Physiologic Tests and Patient Centred Measures of Perceived Dyspnea and Functional Disability. PLoS One 2016;11:e0149240.
16. Agency for Toxic Substances and Disease Registry. Available online: http://www.atsdr.cdc.gov/. Accessed on May 5, 2006.
17. Glazer CS. Acute Inhalational Injury. In: Hanley ME, Welsh CH. editors. Current Diagnosis & Treatment in Pulmonary Medicine. International Ed. New York: Mc-Graw Hill, 2003:354-60.
18. Newman LS, Gottschall EB. Toxic Inhalational Lung

Injury. In: Albert RK, Spiro SG, Jett JR. editors. Clinical Respiratory Medicine. 2nd ed. Philadelphia: Mosby, 2004:759-64.
19. CEC. Quality criteria for computed tomography, European guidelines, EUR l 6262. Luxembourg: Commission of the European Communities, 1999.
20. Ooi GC, Khong PL, Muller NL, et al. Severe acute respiratory syndrome: temporal lung changes at thin-section CT in 30 patients. Radiology 2004;230:836-44.
21. Huuskonen O, Kivisaari L, Zitting A, et al. High-resolution computed tomography classification of lung fibrosis for patients with asbestos-related disease. Scand J Work Environ Health 2001;27:106-12.
22. Gattinoni L, Caironi P, Pelosi P, Goodman LR. What has computed tomography taught us about the acute respiratory distress syndrome? Am J Respir Crit Care Med 2001;164:1701-11.
23. Han XY, Ge Y. CT pulmonary function imaging and its clinical application. J Clin Rehabil Tiss Eng Res 2011;15:753-6.
24. Huang KL, Chen CW, Chu SJ, et al. Systemic inflammation caused by white smoke inhalation in a combat exercise. Chest 2008;133:722-8.
25. Chian CF, Wu CP, Chen CW, et al. Acute respiratory distress syndrome after zinc chloride inhalation: survival after extracorporeal life support and corticosteroid treatment. Am J Crit Care 2010;19:86-90.
26. Hsu HH, Tzao C, Chang WC, et al. Zinc chloride (smoke bomb) inhalation lung injury: clinical presentations, high resolution CT findings, and pulmonary function test results. Chest 2005;127:2064-71.
27. Gil F, Pla A, Hernández AF, et al. A fatal case following exposure to zinc chloride and hexachloroethane from a smoke bomb in a fire simulation at a school. Clin Toxicol (Phila) 2008;46:563-5.
28. Milliken JA, Waugh D, Kadish ME. Acute interstitial pulmonary fibrosis caused by a smoke bomb. Can Med Assoc J 1963;88:36-9.
29. Hjortsø E, Qvist J, Bud MI, et al. ARDS after accidental inhalation of zinc chloride smoke. Intensive Care Med 1988;14:17-24.
30. Holmes PS. Pneumomediastinum associated with inhalation of white smoke. Mil Med 1999;164:751-2.
31. Gapany-Gapanavicius M, Yellin A, Almog S, et al. Pneumomediastinum: a complication of chlorine exposure from mixing household cleaning agents. JAMA 1982;248:349-50.
32. Shulman D, Reshef D, Nesher R, et al. Pulmonary barotrauma including orbital emphysema following inhalation of toxic gas. Intensive Care Med 1988;14:241-3.

Cite this article as: Ma Y, Zhang S, Zhao L, Zhou X, Mao Z, Xu H, Ru X, Huang G. Inhalation lung injury induced by smoke bombs in children: CT manifestations, dynamic evolution features and quantitative analysis. J Thorac Dis 2018;10(10):5860-5869. doi: 10.21037/jtd.2018.09.84

